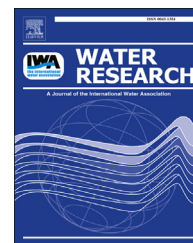


Available online at www.sciencedirect.com

ScienceDirect

journal homepage: www.elsevier.com/locate/watres

Iron colloids reduce the bioavailability of phosphorus to the green alga *Raphidocelis subcapitata*

Stijn Baken*, Sophie Nawara, Christoff Van Moorlegheem, Erik Smolders

KU Leuven, Department of Earth and Environmental Sciences, Kasteelpark Arenberg 20 Bus 2459, 3001 Leuven, Belgium

ARTICLE INFO

Article history:

Received 19 November 2013

Received in revised form

24 March 2014

Accepted 4 April 2014

Available online 18 April 2014

Keywords:

Phosphorus bioavailability

Phosphorus uptake

Ferrihydrite

Colloidal phosphorus

Free phosphorus

Phosphorus sorption

ABSTRACT

Phosphorus (P) is a limiting nutrient in many aquatic systems. The bioavailability of P in natural waters strongly depends on its speciation. In this study, structural properties of iron colloids were determined and related to their effect on P sorption and P bioavailability. The freshwater green alga *Raphidocelis subcapitata* was exposed to media spiked with radiolabelled $^{33}\text{PO}_4$, and the uptake of ^{33}P was monitored for 1 h. The media contained various concentrations of synthetic iron colloids with a size between 10 kDa and $0.45\ \mu\text{m}$. The iron colloids were stabilised by natural organic matter. EXAFS spectroscopy showed that these colloids predominantly consisted of ferrihydrite with small amounts of organically complexed Fe. In colloid-free treatments, the P uptake flux by the algae obeyed Michaelis–Menten kinetics. In the presence of iron colloids at 9 or $90\ \mu\text{M}$ Fe, corresponding to molar P:Fe ratios between 0.02 and 0.17, the truly dissolved P ($<10\ \text{kDa}$) was between 4 and 60% of the total dissolved P ($<0.45\ \mu\text{m}$). These colloids reduced the P uptake flux by *R. subcapitata* compared to colloid-free treatments at the same total dissolved P concentration. However, the P uptake flux from colloid containing solutions equalled that from colloid-free ones when expressed as truly dissolved P. This demonstrates that colloidal P did not contribute to the P uptake flux. It is concluded that, on the short term, phosphate adsorbed to ferrihydrite colloids is not available to the green alga *R. subcapitata*.

© 2014 Elsevier Ltd. All rights reserved.

1. Introduction

In freshwater, the complex speciation of phosphorus (P) and its bioavailability are closely related. The operationally defined “dissolved” ($<0.45\ \mu\text{m}$) fraction of natural waters may contain inorganic, organic, and colloidal P species (Turner et al., 2005). The inorganic P fraction mainly consists of ionic phosphate (orthophosphate, PO_4). Organic P species include,

for example, phytate and adenosine triphosphate (ATP). In addition, P may be adsorbed to or incorporated in colloids such as Fe and Al oxyhydroxide colloids. On average, the P in the dissolved fraction of Flemish freshwaters is predominantly present as colloidal P (52%) and orthophosphate (28%), which highlights the importance of the colloidal P fraction (Van Moorlegheem et al., 2011).

Phosphorus is a limiting nutrient in many freshwater ecosystems, and eutrophication of such systems has often

* Corresponding author. Tel.: +32 16321761.

E-mail address: stijn.baken@ees.kuleuven.be (S. Baken).

<http://dx.doi.org/10.1016/j.watres.2014.04.010>

0043-1354/© 2014 Elsevier Ltd. All rights reserved.

been linked to excessive P inputs (Schindler, 2012). However, the bioavailability of P depends on the P speciation. Algae take up P predominantly in the form of free orthophosphate. Organic and colloidal P species are hydrolysed prior to uptake (Pandey and Parveen, 2011). Hydrolysis might occur either abiotically (due to hydrolytic or photolytic reactions) or biotically (enzymatically). For practical purposes, the bioavailable P is often measured by colorimetric methods and reported as soluble reactive phosphorus (SRP) or dissolved reactive phosphorus (DRP), an approach followed in water quality monitoring programmes worldwide. However, it has been shown that SRP often overestimates the bioavailable P fraction (Boström et al., 1988; Reynolds and Davies, 2001; Rigler, 1968). Apart from free orthophosphate, other P species such as P associated with Fe and Al colloids are also included in the SRP (Hens and Merckx, 2002; Van Moorlegheem et al., 2011), possibly because the acidic colorimetric reagent dissolves such colloids (Sinaj et al., 1998).

The P availability to algae may be measured in various ways, and an operationally defined distinction is made between the immediate and the potential availability (Boström et al., 1988). The immediate or direct P availability is measured by short-term (minutes–hours) experiments, which allow the detection of P influx by means of radioactive tracers. This P fraction is useful for better understanding P dynamics in aquatic systems, especially if the focus is on the dissolved P fraction. In contrast, long-term (days–weeks) experiments in P-limited solutions measure the algal growth response and determine the potential or ultimate availability. The potentially available P fraction comprises both the directly available P and the P that can ultimately be transformed into available forms by biotic or abiotic hydrolysis (Boström et al., 1988).

Both the immediate and the potential P availability are strongly dependent on P speciation. The potential P availability in natural waters may range from 0 to 100% of the total P, depending on the source and, hence, on P speciation (Ekholm and Krogerus, 2003). Free orthophosphate is immediately available, but organic and colloidal P compounds may contribute in varying degrees to the immediate or potential P availability. The availability of organic P is relatively well documented: the immediate availability of most model organic P compounds (e.g. nucleotides, phosphate esters) is below 20%, whereas their potential bioavailability varies widely between 2 and 72%, depending on the compound (Björkman and Karl, 1994; Cotner and Wetzel, 1992; Van Moorlegheem, 2013). Less attention has so far been paid to the availability of colloidal P. Colloidal P might, for instance, be desorbed from the colloid surface and thereby contribute to the P availability. Alternatively, diffusion limited conditions may occur. If desorption of colloidal P is quick and takes place in an unstirred depletion layer adjacent to the cell, colloidal P might enhance the P uptake flux. Such has previously been observed for P uptake by *Brassica napus* roots (Santner et al., 2012). Previous studies on the algal availability of colloidal P have yielded variable and contrasting results (Paerl and Downes, 1978; Van Moorlegheem et al., 2013b; White and Payne, 1980) which emphasizes the need for further exploring the colloidal P fraction. Moreover, to our knowledge, the immediate availability of P in a well-defined model system has never been related to measurements of free P.

This study was set up to measure the immediate (short-term) availability of colloidal orthophosphate to freshwater green algae in a model system. A washed P-starved culture of the freshwater green alga *Raphidocelis subcapitata* was exposed to media containing orthophosphate as the only P-source and either or not containing synthetic iron-organic matter colloids. The P uptake flux, measured using a $^{33}\text{PO}_4$ radiotracer, was used as a proxy for the immediate P availability. It was hypothesized that iron colloids reduce the free P concentration, and thereby also the P availability.

2. Materials and methods

2.1. Test organism and culture conditions

A schematic of the experimental set-up is shown in the Supplementary Material (Fig. SM1). The freshwater green alga *Raphidocelis subcapitata*, formerly known as *Pseudokirchneriella subcapitata* or as *Selenastrum capricornutum*, was selected as the test species. This member of the Chlorophyceae class occurs in nutrient-rich freshwaters (Round, 1981) and has been used extensively in toxicity testing. It has also been used for bioassays for P in freshwaters (Carr and Goulder, 1990; Ekholm, 1994; Ekholm et al., 2003). The procedures for preparing the algae for the experiments are reported in the Supplementary Material. Briefly, a pure culture of *R. subcapitata* was obtained from the Culture Collection of Algae and Protozoa (CCAP 278/4, Oban, U.K.). A subculture was initiated in sterile culture medium (a modified WC medium with adequate P supply; composition: Table 1). The algae were subsequently harvested and starved for P by transferring them to a P-free medium. The P-starved algae were finally washed and suspended in a small volume of P-free medium for use in the uptake experiments. The cell density of this suspension was determined by particle counting (HIAC Royco 9705).

2.2. Test media and treatments

All test media had a uniform background composition (Table 1). Compared to the culture medium, the test media contained less Ca and Mg, no P, no trace metals, and they additionally contained Suwannee River natural organic matter (SRNOM). The Ca and Mg concentrations were reduced in order to avoid flocculation and precipitation of the iron-organic matter colloids. The P and trace metals were removed because they interfered with the P uptake experiment. The SRNOM (International Humic Substances Society) was added in order to stabilise the iron colloids, which otherwise would flocculate.

The test media of different treatments had varying Fe and P concentrations, which are listed in Table 4. The colloid-free treatments did not contain Fe colloids and had free orthophosphate as the only P source. The P was added to the test media 24 h before the start of the experiment as pre-mixed aliquots of $^{31}\text{PO}_4$ (from an orthophosphate standard solution, KH_2PO_4 in H_2O , with a certified PO_4 concentration of 1000 mg L^{-1} , Merck Millipore) and radiolabelled $^{33}\text{PO}_4$ (from $\text{H}_3^{33}\text{PO}_4$ in H_2O , Perkin Elmer). The colloid-containing treatments were prepared by addition of 9 or $90 \text{ } \mu\text{M Fe(II) L}^{-1}$ (as

Table 1 – Composition of the culture medium to grow algae, the P-free medium to induce P starvation, and the test medium (before addition of P and Fe) used in the ^{33}P uptake experiments.

	Culture medium	P-free medium	Test medium	
$\text{CaCl}_2 \cdot 2\text{H}_2\text{O}$	0.25	0.25	0.005	mM
$\text{MgSO}_4 \cdot 7\text{H}_2\text{O}$	0.15	0.15	0.003	mM
NaHCO_3	0.15	0.15	0.15	mM
NaNO_3	1.0	1.0	1.0	mM
$\text{K}_2\text{HPO}_4 \cdot 3\text{H}_2\text{O}$	0.050	x	x	mM
KNO_3	x	0.10	0.10	mM
SRNOM	x	x	10	mg L^{-1}
HEPES buffer	2.0	2.0	2.0	mM
pH	7.5	7.5	7.5	
Ionic strength	3.6	3.6	2.3	mM
$\text{Na}_2\text{H}_2\text{EDTA} + \text{FeCl}_3 \cdot 6\text{H}_2\text{O}$	12	12	x	μM
$\text{CuSO}_4 \cdot 5\text{H}_2\text{O}$	0.040	0.040	x	μM
$\text{ZnSO}_4 \cdot 7\text{H}_2\text{O}$	0.077	0.077	x	μM
$\text{CoCl}_2 \cdot 6\text{H}_2\text{O}$	0.042	0.042	x	μM
$\text{MnCl}_2 \cdot 4\text{H}_2\text{O}$	0.89	0.89	x	μM
$\text{Na}_2\text{MoO}_4 \cdot 2\text{H}_2\text{O}$	0.025	0.025	x	μM
H_3BO_3	16	16	x	μM

x: not present.

SRNOM: Suwannee River natural organic matter.

dissolved $\text{FeSO}_4 \cdot 7\text{H}_2\text{O}$) to the test media 48 h before the start of the experiment. The Fe concentration of 9 μM is within the range commonly encountered in filtered stream water samples, albeit towards the high end (10th–90th percentile 0.14–13 μM Fe, Salminen, 2005), whereas the 90 μM was included because it was anticipated that the effects on P binding would be more easily detected. Oxidation of Fe(II) to Fe(III) occurred within a few hours at pH 7.5 (Davison and Seed, 1983). This yielded iron (hydr)oxides which were in the colloidal size range due to the stabilisation by SRNOM. After 24 h of oxidation, the test media were filtered in order to remove any particulate iron (Chromafil PET-45/25 membrane filters, 0.45 μm pore size, Macherey–Nagel), and the pH was checked and adapted to 7.5. The colloid containing treatments were further subdivided. In the P adsorption treatments, P was added 24 h before the start of the experiment, i.e. after the synthesis of the iron colloids, and therefore the binding of P likely occurred mainly at the surface of the colloids. In the P incorporation treatments P was added just before the addition of the Fe(II), and therefore P binding also occurred by coprecipitation. In all treatments, the $^{33}\text{PO}_4$ was added simultaneously with the $^{31}\text{PO}_4$, and therefore ^{33}P was a perfect tracer for orthophosphate. The activity of ^{33}P in all treatments was approximately 4.5 nCi mL^{-1} .

The total initial P and Fe concentrations in the test media were measured by ICP-MS (Agilent 7700x, limit of quantification was 0.08 μM for P and 0.01 μM for Fe). The “truly dissolved” or “free” P, i.e. the P that was not colloidal, was determined after centrifugal ultrafiltration of the test media (Vivaspin 6 centrifugal concentrator with 10 kDa PES membrane, Sartorius Stedim) and measurement of the ^{33}P activity in the ultrafiltrate by liquid scintillation counting (Tri-Carb 2800TR, Perkin Elmer). Centrifugal ultrafiltration has previously successfully been used for the separation of colloidal from truly dissolved species in environmental samples (Schlosser et al., 2013). Preliminary experiments showed that orthophosphate was not sorbed or retained by the 10 kDa membrane: the recovery of ^{33}P in the ultrafiltrate of colloid-free test media and

of ultrapure water spiked with $^{33}\text{PO}_4$ was >95%. Distribution coefficients (K_D) of P were calculated as the colloidal P concentration (expressed per kg Fe since the exact mass of the colloids is unknown) divided by the free P concentration.

2.3. Speciation of the iron colloids

Two samples of the synthetic colloids used in the uptake experiment were prepared for measurement of the size distribution and EXAFS (Extended X-ray Absorption Fine Structure) spectroscopy. These samples contained the same background composition as the test media and contained nominal Fe additions of 90 μM Fe (corresponding to 9000 $\mu\text{mol Fe (g SRNOM)}^{-1}$; sample A) and 9 μM Fe (corresponding to 900 $\mu\text{mol Fe (g SRNOM)}^{-1}$; sample B). They did not contain P, but since the colloids in the algal experiments contained at most 0.1 mol P (mol Fe) $^{-1}$, it is unlikely that P would affect the Fe speciation in the colloids to a large extent. The size distribution of Fe was measured by ICP-MS after 24 h of oxidation and after filtration of the test media over 0.45 μm membrane filters (Chromafil PET-45/25), 0.1 μm membrane filters (Acrodisc filters with Supor membrane, Pall Life Sciences), and 10 kDa ultrafiltration concentrators (Vivaspin 6). The Fe(II) concentration in these samples was measured with the ferrozine method (Viollier et al., 2000).

Freeze-dried subsamples of the colloidal samples A and B were measured by Fe-edge (7112 eV) EXAFS spectroscopy at the wiggler beamline I811, MAX-lab, Lund, Sweden. Standard spectra of 2-line ferrihydrite and Fe complexed by SRNOM (90 $\mu\text{mol Fe (g SRNOM)}^{-1}$) were also measured, and standard spectra of goethite, lepidocrocite, and the Fe(III)-trioxalate complex were obtained from earlier studies (Kleja et al., 2012; Sjöstedt et al., 2013; van Schaik et al., 2008). The EXAFS spectra were analysed by wavelet transforms (WT), linear combination fitting (LCF), and conventional EXAFS modelling. For the traditional EXAFS modelling, a model similar to those used in Mikutta (2011) and Baken et al. (2013) was used. The

model included single scattering Fe–O and multiple scattering Fe–O–O interactions in the first coordination shell, a single scattering Fe–Fe₂ interaction in the second coordination shell, and a single scattering Fe–Fe₃ interaction in the third coordination shell. This model contained a total of 14 parameters, 7 of which were fixed or constrained (Table 3). Further details on the measurement and analysis of EXAFS spectra are given in the [Supplementary Material](#).

2.4. Uptake experiment

The short-term P uptake experiment was conducted as described by [Van Moorlegghem et al. \(2013a\)](#). One single culture of *R. subcapitata* was used with an internal P content of 0.4%. The experiment was carried out in triplicate in acid washed 100-mL beakers, each containing 15 mL of test medium. The beakers were placed on an unshaken light cabinet under ambient conditions. Aliquots of the washed P-starved algae culture (see Section 2.1) were added to the test media to yield a final cell density of 5×10^5 cells mL⁻¹. The addition of the algae marked the start of the experiment.

Approximately 5, 30, and 60 min after the addition of the algae, 1-mL samples were transferred into Eppendorf tubes and immediately centrifuged (15 min, 6000 g) in order to separate the algae from the test medium. The supernatant was removed, the remaining pellet was suspended in 1 mL of ultrapure water, and the ³³P activity in both fractions was measured by liquid scintillation counting (Tri-carb 2800TR, Perkin Elmer) after the addition of 2 mL scintillation cocktail (Ultima Gold, Perkin Elmer). The recovery of ³³P in the pellet and in the supernatant was always between 96 and 103% of the total ³³P in the test medium. The algal pellet was not washed because earlier experiments using various washing media showed that no extracellular phosphate could be removed ([Van Moorlegghem et al., 2013a](#)). Preliminary tests also showed that, under the conditions of this experiment (i.e. low concentrations of divalent cations in the test media), very little adsorption of colloids onto the surface of algal cells or precipitation of colloids during the centrifugation step occurred: the loss of Fe from the supernatant after centrifugation was on average 3% (and never more than 7%) compared to the Fe initially present. It could therefore be assumed that all ³³P recovered in the pellet was internalised by the algae.

2.5. Calculations

The internalised ³³P fraction in each sample, ³³P_{int}, was calculated by dividing the ³³P activity in the pellet by the total ³³P activity. A simple linear regression model was fitted to the data of ³³P_{int} versus time ($n = 9$) using a least-squares algorithm. The slope of this linear model represented the ³³P internalisation flux by the algae. Since the ³³P was a perfect tracer for orthophosphate, the slope of this regression model could be converted to the P uptake flux, expressed as P influx per unit cell surface, F_P , using the equation

$$F_P = {}^{33}\text{P}_{\text{int}} \cdot [\text{P}] \cdot \frac{1}{A \cdot C}$$

where ³³P_{int} is the internalised ³³P fraction, [P] is the initial total P concentration in the test medium (as measured by ICP-

MS), A is the average surface area of *R. subcapitata* cells which is 67 μm² cell⁻¹ ([Weiner et al., 2004](#)), and C is the cell density of *R. subcapitata* in the experiment which equalled 5×10^5 cells mL⁻¹. The P uptake flux, F_P , is in this experiment used as a measure of the immediate P bioavailability.

In colloid-free treatments, the uptake fluxes were fitted using a Michaelis-Menten-type equation:

$$F_P = F_{\text{MAX}} \frac{[\text{PO}_4]}{K_M + [\text{PO}_4]}$$

with F_{MAX} the uptake flux at saturation, K_M the half-saturation constant, and $[\text{PO}_4]$ the orthophosphate concentration in the test medium measured as P concentration by ICP-MS. Parameter optimisation, calculation of interpolated values, and their estimated standard errors and 95% confidence limits were performed using a nonlinear least squares algorithm (the NLIN procedure) in SAS 9.3.

3. Results and discussion

3.1. Speciation of the iron colloids

The majority of the Fe added to the test media was recovered in the fraction between 0.1 μm and 10 kDa (Table 2). The latter roughly corresponds to a hydrodynamic diameter between 1 and 2 nm ([Erickson, 2009](#)). This confirms that the Fe was predominantly present in the colloidal fraction. The Fe in the colloidal fraction was partly (8–23%) still present as reduced Fe(II), and is likely Fe(II) bound by SRNOM or by the iron colloids. The near absence of truly dissolved Fe(II), i.e. Fe(II) in the <10 kDa fraction, indicates that the oxidation process was completed after 24 h as expected from earlier studies ([Davison and Seed, 1983](#)). Preliminary experiments revealed that, in the absence of SRNOM, the Fe readily flocculated and settled, which suggests that the SRNOM stabilised the Fe-colloids. This is in agreement with earlier studies which have shown that colloidal Fe strongly interacts with and may be stabilised by natural organic matter ([Gaffney et al., 2008](#); [Pédrot et al., 2011](#)).

The EXAFS spectrum of the colloidal sample A (9000 μmol Fe (g SRNOM)⁻¹) strongly resembles that of ferrihydrite, whereas that of the colloidal sample B (900 μmol Fe (g SRNOM)⁻¹) shows resemblance to both the ferrihydrite and the Fe-SRNOM complex (Fig. 1). The wavelet transform plots (Supplementary Material, Fig. SM2) of both colloidal samples confirm the presence of Fe–Fe interactions as evidenced by the pronounced maximum around $k = 7 \text{ \AA}^{-1}$ and $R = 2.8 \text{ \AA}$. Such Fe–Fe interactions are absent from the wavelet transform plots of the Fe-SRNOM complex standard, confirming that the Fe in this standard was indeed present as organic complexes and that it was not hydrolysed. The linear combination fitting results confirm that ferrihydrite was the predominant constituent of both colloidal samples. Depending on the k -range used, the colloidal sample A was fitted as 83–87% ferrihydrite, 7–9% lepidocrocite, 2–8% Fe-SRNOM complex, and <3% of goethite and Fe-oxalate complex. The colloidal sample B was fitted as 63–83% ferrihydrite, 7–33% Fe-SRNOM complex, and <3% of the other standards. Especially for sample B, the fitted fraction of Fe-SRNOM strongly

Table 2 – Speciation and size distribution of Fe in the synthetic colloids (all data in $\mu\text{M Fe}$).

Sample	Unfiltered		<0.45 μm		<0.1 μm		<10 kDa	
	Fe	Fe(II)	Fe	Fe(II)	Fe	Fe(II)	Fe	Fe(II)
Colloids A: 9000 $\mu\text{mol Fe (g SRNOM)}^{-1}$	86.3	7.3	84.3	7.3	72.5	6.1	0.7	0.4
Colloids B: 900 $\mu\text{mol Fe (g SRNOM)}^{-1}$	8.8	2.3	8.6	2.1	7.9	1.8	1.1	0.4

depended on the k -range used and increased as the higher limit of the k -range increased. This reflects the uncertainty associated with the LCF method. The EXAFS spectra of the iron colloids and that of ferrihydrite were fitted well by the proposed model with Fe–Fe interactions in the second and third coordination shells around 3.05 and 3.43 Å (Fig. 1 and Table 3). The former distance refers to edge-sharing Fe octahedra, whereas the latter refers to corner-sharing octahedra (Manceau and Drits, 1993). The inclusion of a triangular multiple scattering path (Fe–O–O) significantly improved the model fits as evidenced by a lower chi-squared statistic. The Fe–Fe interactions in sample A were more pronounced than those in sample B, as reflected by the higher coordination numbers. Even though the LCF analysis suggested the

presence of Fe-organic complexes, no Fe–C interactions could be refined in either colloidal sample. Since C is a much lighter element than Fe, Fe–C interactions are easily overshadowed by Fe–Fe interactions (Sjöstedt et al., 2013).

The EXAFS spectra and the refined Fe–Fe distances in our samples agree well with naturally occurring ferrihydrite (Cismasu et al., 2011) and with previous studies on Fe and SRNOM (Karlsson and Persson, 2012). Upon oxidation of Fe(II) in near-neutral waters, the expected reaction product may be a hydrous ferric oxide with few corner-sharing Fe–Fe linkages, 2-line ferrihydrite, or lepidocrocite, depending on the Si concentrations (Mayer and Jarrell, 2000; Voegelin et al., 2010). The Si concentrations in our test media (around 7 $\mu\text{M Si L}^{-1}$) are in the range where ferrihydrite formation can be expected.

Table 3 – Optimal parameter values and uncertainties for the R-space fits of EXAFS spectra of synthetic iron colloids and ferrihydrite.

Sample	Red χ^2	S_0^{2a}	E_0 (eV)	Fe–O ^b		Fe–Fe ₂ ^c		Fe–Fe ₃ ^c		Fe–O–O ^d
				R (Å)	σ^2 (Å ²)	N	R (Å)	N	R (Å)	
Ferrihydrite	469	0.78*	0.34 ± 0.51	1.98 ± 0.01	0.0112 ± 0.0004	2.7 ± 0.4	3.05 ± 0.01	1.5 ± 0.4	3.44 ± 0.02	$3.38 \pm 0.01^*$
Colloids A: 9000 $\mu\text{mol Fe (g SRNOM)}^{-1}$	365	0.78*	0.63 ± 0.51	1.98 ± 0.01	0.0089 ± 0.0004	3.6 ± 0.5	3.06 ± 0.01	1.8 ± 0.4	3.43 ± 0.02	$3.38 \pm 0.01^*$
Colloids B: 900 $\mu\text{mol Fe (g SRNOM)}^{-1}$	117	0.78*	1.33 ± 0.54	1.99 ± 0.01	0.0090 ± 0.0005	2.5 ± 0.7	3.07 ± 0.02	1.4 ± 0.6	3.43 ± 0.03	$3.40 \pm 0.01^*$

Red χ^2 : reduced chi-square statistic; S_0^2 : passive amplitude reduction factor; E_0 : edge energy; R: half path length; σ^2 : Debye-Waller factor; N: degeneracy; *: constrained parameter.

^a S_0^2 was set to 0.78 which was obtained from a first-shell fit of ferrihydrite between $R = 1.0$ and 2.0 Å and with N set to 6.

^b N of the Fe–O path was set to 6.

^c σ^2 of the Fe–Fe paths was set to 0.014 Å² for the Fe–Fe₂ path and to 0.009 Å² for the Fe–Fe₃ path. These values were derived from a fit of ferrihydrite between $R = 2.0$ and 4.0 Å while keeping the first shell parameters fixed.

^d For the Fe–O–O multiple scattering path, N was set to 24, R was constrained to equal 1.707 times that of the Fe–O path, and σ^2 was constrained to equal that of the Fe–O path.

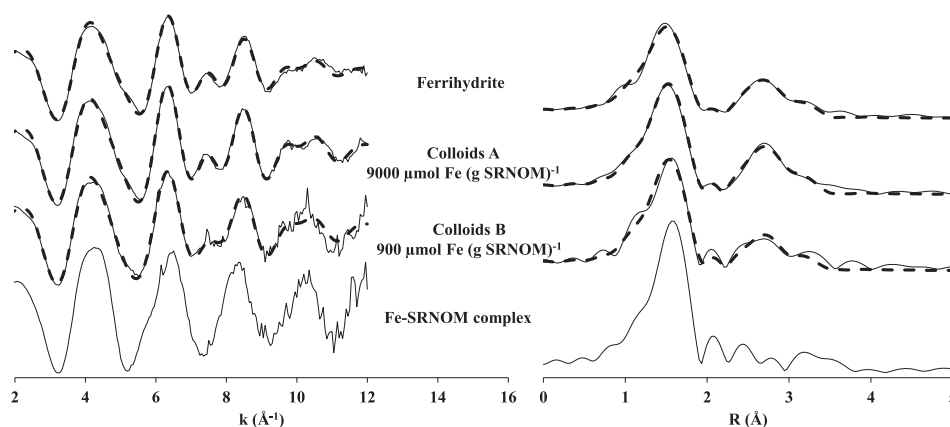


Fig. 1 – k^3 -weighted Fe EXAFS spectra (left) and their Fourier transforms (right) of ferrihydrite, synthetic iron colloids, and Fe complexed by Suwannee River NOM. Full lines are observed data; dashed lines are model fits.

Table 4 – Flux of P uptake by *R. subcapitata* at different P concentrations and with or without iron colloids. In colloid-free treatments, the total P equalled the free P concentration, which is operationally defined as <10 kDa. In P adsorption treatments, P was added after the oxidation of ferrous iron and the formation of iron colloids. In P incorporation treatments, P was added before the addition of ferrous iron. The distribution coefficient K_D is defined as the colloidal P concentration (expressed per unit Fe) divided by the free P concentration.

Treatment	Treatment type	Fe	Total P	P:Fe	Free P (<10 kDa)		K _D 10 ⁶ L (kg Fe) ⁻¹	Uptake flux (pmol P cm ⁻² s ⁻¹) ± 95% confidence limits		
		μM	μM	mol:mol	μM	%		Observed	Predicted from total P	Predicted from free P
1	Colloid-free	0.5	0.6		0.6	100	x	0.10 ± 0.01	0.13 ± 0.03	
2	Colloid-free	0.5	0.9		0.9	100	x	0.21 ± 0.03	0.20 ± 0.04	
3	Colloid-free	0.5	1.5		1.5	100	x	0.26 ± 0.02	0.30 ± 0.06	
4	Colloid-free	0.5	3.5		3.5	100	x	0.62 ± 0.04	0.60 ± 0.09	
5	Colloid-free	0.5	5.9		5.9	100	x	0.78 ± 0.07	0.85 ± 0.09	
6	Colloid-free	0.5	9.6		9.6	100	x	1.22 ± 0.11	1.12 ± 0.09	
7	Colloid-free	0.5	26.3		26.3	100	x	1.58 ± 0.31	1.61 ± 0.16	
8	P adsorption	80.4	1.7	0.02	0.5	27	0.6	0.14 ± 0.01	0.35 ± 0.07	0.11 ± 0.02
9	P adsorption	84.9	3.6	0.04	1.9	52	0.2	0.40 ± 0.09	0.62 ± 0.09	0.37 ± 0.07
10	P incorporation	7.9	0.9	0.11	0.5	53	2.0	0.09 ± 0.01	0.19 ± 0.04	0.11 ± 0.02
11	P incorporation	7.5	1.1	0.15	0.6	55	1.9	0.14 ± 0.01	0.23 ± 0.05	0.13 ± 0.03
12	P incorporation	8.1	1.4	0.17	0.8	60	1.5	0.16 ± 0.03	0.28 ± 0.06	0.18 ± 0.04
13	P incorporation	81.8	2.8	0.03	0.1	4	5.3	0.02 ± 0.01	0.51 ± 0.08	0.03 ± 0.01
14	P incorporation	84.5	9.7	0.12	0.6	6	3.2	0.10 ± 0.06	1.12 ± 0.09	0.13 ± 0.03

It is concluded that the colloids predominantly consisted of ferrihydrite with small amounts of lepidocrocite (sample A) and Fe-organic complexes.

3.2. Binding of orthophosphate by the iron colloids

Orthophosphate was quickly and efficiently bound by the iron colloids, as evidenced by the high K_D values of P binding, which are in the range of 10^5 – $10^6 \text{ L (kg Fe)}^{-1}$ (Table 4). The colloids contained between 0.01 and 0.1 mol P (mol Fe) $^{-1}$. The free (truly dissolved, i.e. < 10 kDa) P concentration was between 4 and 60%. In the adsorption treatments, to which the P was added after the formation of the iron colloids, the P had roughly 10-fold lower K_D values than in similar incorporation treatments, in which P was present during the formation of the iron colloids. This is in good agreement with Mayer and Jarrell (2000): P binding by Si-containing Fe hydroxides is stronger if the P is present during their formation. Voegelin et al. (2013, 2010) showed that, upon oxidation of Fe(II) at pH 7 in the presence of phosphate, a Fe-phosphate phase is formed as long as dissolved phosphate is present. Therefore, the P binding in the incorporation treatments likely occurred through coprecipitation of Fe and P. Other earlier work on environmental samples has also demonstrated high P binding by freshly formed Fe(III) colloids and precipitates (Gunnars et al., 2002; Lienemann et al., 1999).

3.3. P uptake flux by *R. subcapitata*

In all treatments, the increase in internalised ^{33}P fraction with time was linear between 5 and 60 min after the start of the experiment (Supplementary Material, Fig. SM3). The slope of the linear regression model was converted to the P uptake flux (Table 4). The P uptake flux of treatments 13 and 14 had relatively wide confidence limits compared to the other treatments, which was due to the low internalised ^{33}P activity in these treatments. The concept of a constant P uptake flux is based on the assumptions of a one-step internalisation and a constant external P concentration. It may not accurately reflect the actual uptake process (Yao et al., 2011), but has proven satisfactory for algal P uptake in a wide range of studies. The 60-min interval was selected based on preliminary tests, which showed that the ^{33}P internalisation levelled off after 120 min. At high P concentrations, the amount of internalised P after 120 min was around 0.5% on a dry weight basis, suggesting that the algae had reached an adequate internal P concentration and that feedback mechanisms likely caused a reduced P uptake flux (Van Moorleghe et al., 2013a). Conversely, in the treatments with low (<2 μM) free P concentrations, the deviation from linearity was likely due to the decrease in solution P concentration, which was up to 70% after 120 min. The uptake of P was not limited by diffusion of P towards the cell surface. The maximum diffusion flux to a spherical cell was estimated using the equation of Schulz and Jørgensen (2001) assuming a cell radius of $R = 5 \text{ μm}$, a bulk P concentration of $C = 0.5 \text{ μM}$, a cell surface P concentration of zero, and a diffusivity of P in water of $D = 10^{-5} \text{ cm}^2 \text{ s}^{-1}$. The predicted maximum diffusion flux to the surface of the sphere is $D \cdot C \cdot R^{-1} = 10 \text{ pmol cm}^{-2} \text{ s}^{-1}$, which

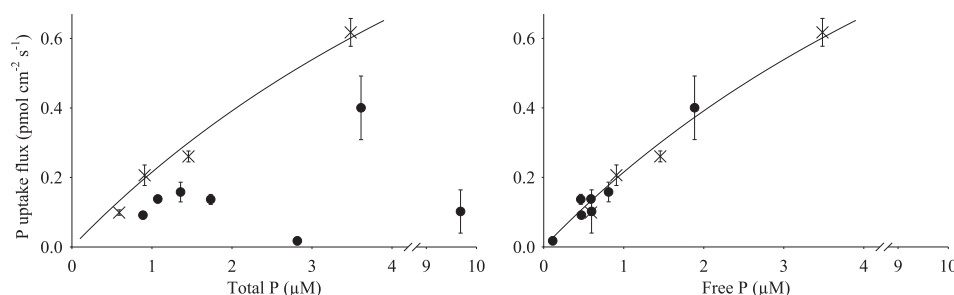


Fig. 2 – Phosphorus uptake flux in colloid-free (crosses) and colloid-containing (closed circles) treatments plotted versus total (left) and free (< 10 kDa; right) P concentrations. The full line is the Michaelis–Menten equation fitted to the colloid-free treatments. Error bars represent 95% confidence limits.

exceeds the fluxes observed in our experiment by more than an order of magnitude. Even though the assumption of spherical cells is flawed for *R. subcapitata*, it is unlikely that P uptake by starved *R. subcapitata* cells was diffusion limited.

In the colloid-free treatments, i.e. with free orthophosphate as the only P source, the P uptake flux obeyed Michaelis–Menten kinetics (all data in Table 4, data at low P concentrations plotted in Fig. 2). The Michaelis–Menten parameters fitted to all colloid-free treatments (between 0.6 and 26 μM P) and their estimated standard errors were: $K_M = 9.1 \pm 1.4 \mu\text{M}$ and $F_{\text{MAX}} = 2.2 \pm 0.2 \text{ pmol cm}^{-2} \text{ s}^{-1}$. The F_{MAX} is in the range of values previously encountered for Chlorophyceae, whereas the K_M is slightly above that range (Cembella et al., 1984).

In the colloid-containing treatments, the observed P uptake flux was lower than that in colloid-free treatments with similar total P concentrations (Fig. 2). However, if plotted against free P concentrations, the colloid-containing treatments coincide with the Michaelis–Menten curve (Fig. 2). In other words, the P uptake flux in a medium containing colloids equalled that in a hypothetical colloid-free medium with the same free P concentration. The Michaelis–Menten equation fitted to the colloid-free treatments was used to predict the P uptake flux in colloid-containing treatments. Two types of predictions were made: one using the total P concentration, and another using the free P concentration (Table 4). The predictions based on the total P concentrations exceed the observed values by factors between 1.5 and 30. The predictions based on the free P concentrations are between 0.8 and 1.5 times the observed values (average 1.1, standard error 0.1). The above shows that the colloidal P did not contribute to the P uptake flux and was therefore not immediately available under the conditions of this experiment.

Our findings are in line with earlier work on algal growth response which indicated no or limited long-term (ultimate) algal availability of P adsorbed to synthetic Fe colloids (Van Moorerghem et al., 2013b). However, that study used very large colloid concentrations, and a quantitative analysis was hampered by a lack of separating the free P fraction from the colloidal P. We did not observe diffusion limited uptake, which is in contrast with earlier work on P uptake by plant roots (Santner et al., 2012). This difference is not explained by size effects: the radius of root hairs is typically a few μm

(Vandamme, 2013), i.e. in the same range as the size of *R. subcapitata* cells. Part of the difference may be due to the fact that the algal cells are distributed uniformly in the test media, whereas root hairs are not, which may cause local P depletion in the vicinity of the roots. However, the difference is most likely explained by different free P concentrations (0.01–0.02 μM in the plant uptake experiment versus 0.1–2 μM in this study), which cause a larger diffusive flux towards the cell surface.

The orthophosphate concentrations in European streams commonly range between 0.1 and 4.2 μM (P_{10} – P_{90}) with a median value of 0.8 μM (data for 2010, European Environment Agency EEA, 2013). The P concentrations used in this study are highly representative of those typically encountered in streams. Therefore, the results of this study, which showed that P uptake was not diffusion limited, may be of great relevance for algal uptake of P in stream water. However, some uncertainties remain. Diffusion limited P uptake by biota may, however, occur in streams with very low free P concentrations. Moreover, our test species had a relatively low P uptake rate (Cembella et al., 1984), and colloidal P may be more available to other biological species with very high P uptake rates. Under such conditions, colloidal P may still contribute to the P uptake flux. Furthermore, it is unclear whether colloidal P may to some extent be available on the longer term, e.g. through desorption of P from colloidal surfaces. These issues warrant further studies on the availability of the colloidal P fraction.

4. Conclusions

- Ferrihydrite colloids bind orthophosphate very effectively, and thereby reduce the free (<10 kDa) orthophosphate concentration.
- Such colloids also reduce the bioavailability of P: the short-term (1 h) P uptake flux by a freshwater green alga is lower in test media containing colloidal ferrihydrite than in colloid-free test media at the same total P concentration. However, if only the free orthophosphate fraction is considered, the P uptake flux in test media containing colloidal ferrihydrite equals that in colloid-free media.
- Free orthophosphate is immediately available to biota, but colloidal P is not.

Acknowledgements

Thanks to Peter Salaets and Kristin Coorevits for technical assistance. S.B. thanks the Research Foundation Flanders (FWO) for a PhD fellowship. The EXAFS measurements were carried out at beamline I811, MAX-lab synchrotron radiation source, Lund University, Sweden. Funding for beamline I811 was provided by The Swedish Research Council and The Knut and Alice Wallenberg Foundation. Thanks also to Jon Petter Gustafsson, Carin Sjöstedt, Ingmar Persson, and the beamline I811 staff.

Appendix A. Supplementary data

Supplementary data related to this article can be found at <http://dx.doi.org/10.1016/j.watres.2014.04.010>.

REFERENCES

- Baken, S., Sjöstedt, C., Gustafsson, J.P., Seuntjens, P., Desmet, N., De Schutter, J., Smolders, E., 2013. Characterisation of hydrous ferric oxides derived from iron-rich groundwaters and their contribution to the suspended sediment of streams. *Appl. Geochem.* 39, 59–68.
- Björkman, K., Karl, D., 1994. Bioavailability of inorganic and organic phosphorus compounds to natural assemblages of microorganisms in Hawaiian coastal waters. *Mar. Ecol. Prog. Ser.* 111, 265–273.
- Boström, B., Persson, G., Broberg, B., 1988. Bioavailability of different phosphorus forms in freshwater systems. *Hydrobiologia* 170, 133–155.
- Carr, O.J., Goulder, R., 1990. Fish-farm effluents in rivers—II. Effects on inorganic nutrients, algae and the macrophyte *Ranunculus penicillatus*. *Water Res.* 24, 639–647.
- Cembella, A.D., Antia, N.J., Harrison, P.J., 1984. The utilization of inorganic and organic phosphorous compounds as nutrients by eukaryotic microalgae: a multidisciplinary perspective: part 1. *Crit. Rev. Microbiol.* 10, 317–391.
- Cismasu, A.C., Michel, F.M., Tcaciuc, A.P., Tyliszczak, T., Brown, G.E., 2011. Composition and structural aspects of naturally occurring ferrihydrite. *Comptes Rendus Geosci.* 343, 210–218.
- Cotner, J.B., Wetzel, R.G., 1992. Uptake of dissolved inorganic and organic phosphorus compounds by phytoplankton and bacterioplankton. *Limnol. Oceanogr.* 37, 232–243.
- Davison, W., Seed, G., 1983. The kinetics of the oxidation of ferrous iron in synthetic and natural waters. *Geochim. Cosmochim. Acta* 47, 67–79.
- Ekholm, P., 1994. Bioavailability of phosphorus in agriculturally loaded rivers in southern Finland. *Hydrobiologia* 287, 179–194.
- Ekholm, P., Krogerus, K., 2003. Determining algal-available phosphorus of differing origin: routine phosphorus analyses versus algal assays. *Hydrobiologia* 492, 29–42.
- Ekholm, P., Rita, H., Pitkänen, H., Rantanen, P., Pekkarinen, J., Münster, U., 2003. Algal-available phosphorus entering the Gulf of Finland as estimated by algal assays and chemical analyses. *J. Environ. Qual.* 38, 2322–2333.
- Erickson, H.P., 2009. Size and shape of protein molecules at the nanometer level determined by sedimentation, gel filtration, and electron microscopy. *Biol. Proced. Online* 11, 32–51.
- European Environment Agency EEA, 2013. Waterbase. Online: [WWW Document]. URL: <http://www.eea.europa.eu/data-and-maps/data/waterbase-rivers-9> (accessed 19.11.13.).
- Gaffney, J.W., White, K.N., Boulton, S., 2008. Oxidation state and size of Fe controlled by organic matter in natural waters. *Environ. Sci. Technol.* 42, 3575–3581.
- Gunnars, A., Blomqvist, S., Johansson, P., Andersson, C., 2002. Formation of Fe(III) oxyhydroxide colloids in freshwater and brackish seawater, with incorporation of phosphate and calcium. *Geochim. Cosmochim. Acta* 66, 745–758.
- Hens, M., Merckx, R., 2002. The role of colloidal particles in the speciation and analysis of “dissolved” phosphorus. *Water Res.* 36, 1483–1492.
- Karlsson, T., Persson, P., 2012. Complexes with aquatic organic matter suppress hydrolysis and precipitation of Fe(III). *Chem. Geol.* 322–323, 19–27.
- Kleja, D.B., van Schaik, J.W.J., Persson, I., Gustafsson, J.P., 2012. Characterization of iron in floating surface films of some natural waters using EXAFS. *Chem. Geol.* 326–327, 19–26.
- Lienemann, C.-P., Monnerat, M., Dominik, J., Perret, D., 1999. Identification of stoichiometric iron-phosphorus colloids produced in a eutrophic lake. *Aquat. Sci.* 61, 133.
- Manceau, A., Drits, V.A., 1993. Local structure of ferrihydrite and ferroxhyte by EXAFS spectroscopy. *Clay Min.* 28, 165–184.
- Mayer, T.D., Jarrell, W.M., 2000. Phosphorus sorption during iron(II) oxidation in the presence of dissolved silica. *Water Res.* 34, 3949–3956.
- Mikutta, C., 2011. X-ray absorption spectroscopy study on the effect of hydroxybenzoic acids on the formation and structure of ferrihydrite. *Geochim. Cosmochim. Acta* 75, 5122–5139.
- Paerl, H.W., Downes, M.T., 1978. Biological availability of low versus high molecular weight reactive phosphorus. *J. Fish. Res. Board Can.* 35, 1639–1643.
- Pandey, V.D., Parveen, S., 2011. Alkaline phosphatase activity in cyanobacteria: physiological and ecological significance. *Indian J. Fundam. Appl. Life Sci.* 1, 295–303.
- Pédrot, M., Le Boudec, A., Davranche, M., Dia, A., Henin, O., 2011. How does organic matter constrain the nature, size and availability of Fe nanoparticles for biological reduction? *J. Colloid Interface Sci.* 359, 75–85.
- Reynolds, C.S., Davies, P.S., 2001. Sources and bioavailability of phosphorus fractions in freshwaters: a British perspective. *Biol. Rev. Camb. Philos. Soc.* 76, 27–64.
- Rigler, F.H., 1968. Further observations inconsistent with the hypothesis that the molybdenum blue method measures orthophosphate in lake water. *Limnol. Oceanogr.* 13, 7–13.
- Round, F.E., 1981. *The Ecology of Algae*. Cambridge University Press, Cambridge, U.K.
- Salminen, R. (Ed.), 2005. *Geochemical Atlas of Europe. Part 1: Background Information, Methodology and Maps*. Geological Survey of Finland, Espoo, Finland.
- Santner, J., Smolders, E., Wenzel, W.W., Degryse, F., 2012. First observation of diffusion-limited plant root phosphorus uptake from nutrient solution. *Plant. Cell Environ.* 35, 1558–1566.
- Schindler, D.W., 2012. The dilemma of controlling cultural eutrophication of lakes. *Proc. Biol. Sci.* 279, 4322–4333.
- Schlosser, C., Streu, P., Croot, P.L., 2013. Vivaspin ultrafiltration: a new approach for high resolution measurements of colloidal and soluble iron species. *Limnol. Oceanogr. Meth.* 11, 187–201.
- Schulz, H.N., Jørgensen, B.B., 2001. Big bacteria. *Annu. Rev. Microbiol.* 55, 105–137.
- Sinaj, S., Mächler, F., Frossard, E., Fäisse, C., Oberson, A., Morel, C., 1998. Interference of colloidal particles in the determination of orthophosphate concentrations in soil water extracts. *Commun. Soil Sci. Plant Anal.* 29, 1091–1105.
- Sjöstedt, C., Persson, I., Hesterberg, D., Kleja, D.B., Borg, H., Gustafsson, J.P., 2013. Iron speciation in soft-water lakes and

- soils as determined by EXAFS spectroscopy and geochemical modelling. *Geochim. Cosmochim. Acta* 105, 172–186.
- Turner, B.L., Frossard, E., Baldwin, D.S., 2005. *Organic Phosphorus in the Environment*. CABI Publishing, Wallingford, U.K.
- Van Moorleghem, C., 2013. Detection of Bioavailable Phosphorus Forms for the Alga *Pseudokirchneriella subcapitata*.
- Van Moorleghem, C., De Schutter, N., Smolders, E., Merckx, R., 2013a. Bioavailability of organic phosphorus to *Pseudokirchneriella subcapitata* as affected by phosphorus starvation: an isotope dilution study. *Water Res.* 47, 3047–3056.
- Van Moorleghem, C., Schutter, N., Smolders, E., Merckx, R., 2013b. The bioavailability of colloidal and dissolved organic phosphorus to the alga *Pseudokirchneriella subcapitata* in relation to analytical phosphorus measurements. *Hydrobiologia* 709, 41–53.
- Van Moorleghem, C., Six, L., Degryse, F., Smolders, E., Merckx, R., 2011. Effect of organic P forms and P present in inorganic colloids on the determination of dissolved P in environmental samples by the diffusive gradient in thin films technique, ion chromatography, and colorimetry. *Anal. Chem.* 83, 5317–5323.
- Van Schaik, J.W.J., Persson, I., Kleja, D.B., Gustafsson, J.P., 2008. EXAFS study on the reactions between iron and fulvic acid in acid aqueous solutions. *Environ. Sci. Technol.* 42, 2367–2373.
- Vandamme, E., 2013. Phosphorus-efficient Soybean Germplasm as an Entry Point to Integrated Soil Fertility Management in Western Kenya. KU Leuven.
- Viollier, E., Inglett, P.W., Hunter, K., Roychoudhury, A.N., Van Cappellen, P., 2000. The ferrozine method revisited: Fe(II)/Fe(III) determination in natural waters. *Appl. Geochem.* 15, 785–790.
- Voegelin, A., Kaegi, R., Frommer, J., Vantelon, D., Hug, S.J., 2010. Effect of phosphate, silicate, and Ca on Fe(III)-precipitates formed in aerated Fe(II)- and As(III)-containing water studied by X-ray absorption spectroscopy. *Geochim. Cosmochim. Acta* 74, 164–186.
- Voegelin, A., Senn, A.-C., Kaegi, R., Hug, S.J., Mangold, S., 2013. Dynamic Fe-precipitate formation induced by Fe(II) oxidation in aerated phosphate-containing water. *Geochim. Cosmochim. Acta* 117, 216–231.
- Weiner, J.A., DeLorenzo, M.E., Fulton, M.H., 2004. Relationship between uptake capacity and differential toxicity of the herbicide atrazine in selected microalgal species. *Aquat. Toxicol.* 68, 121–128.
- White, E., Payne, G., 1980. Distribution and biological availability of reactive high molecular weight phosphorus in natural waters in New Zealand. *Can. J. Fish. Aquat. Sci.* 37, 664–669.
- Yao, B., Xi, B., Hu, C., Huo, S., Su, J., Liu, H., 2011. A model and experimental study of phosphate uptake kinetics in algae: considering surface adsorption and P-stress. *J. Environ. Sci.* 23, 189–198.